Probing the Upper Limit of Nonclassical Rotational Inertia

Ann Sophie C. Rittner* and John D. Reppy
Laboratory of Atomic and Solid State Physics and the Cornell Center for Materials Research, Cornell University, Ithaca, New York 14853-2501
(Dated: July 14, 2008)

We study the effect of confinement on solid ^{4}He's nonclassical rotational inertia (NCRI) in a torsional oscillator by constraining it to narrow annular cells of various widths. The NCRI exhibits a broad maximum value of 20% for annuli of ~ 100 μm width. Samples constrained to porous media or to larger geometries both have smaller NCRI, mostly below ~ 1%. In addition, we extend Kim and Chan's blocked annulus experiment to solid samples with large supersolid fractions. Blocking the annulus suppresses the nonclassical decoupling from 17.1% below the limit of our detection of 0.8%. This result demonstrates the nonlocal nature of the supersolid phenomena. At 20 mK, NCRI depends on velocity history showing a closed hysteresis loop in different thin annular cells.

PACS numbers: 66.30.Ma, 67.80.bd

Kim and Chan (KC) have observed an anomalous decrease in solid ^{4}He's rotational inertia below 200 mK in a torsional oscillator [1, 2]. The possibility of a new "super" state of matter sparked a flurry of experimental and theoretical work. When an annular cell is blocked, the nonclassical rotational inertia (NCRI) is strongly reduced [2], indicating that superflow is responsible for the NCRI. To date, the blocked-annulus experiment is the strongest experimental evidence supporting superflow over other explanations as unusual temperature dependence of the elastic properties of the solid [2]. Further support for superflow is that the oscillation frequency has no impact on the signal size [3]. The NCRI has been confirmed in several laboratories [4, 5] with supersolid fractions ranging from 0.03% up to 20% [6]. The supersolid fraction can be altered by experimental parameters such as ^{3}He impurity concentration [1], thermal history of the sample [5], sample pressure, and geometric confinement [6]. Notably, the supersolid fraction increases by more than three orders of magnitude when thin annular geometries confine the sample. From experimental observations and a number of theoretical studies, there has been a growing consensus in the field that crystalline defects are crucial to at least enhance NCRIs (for a review see [7]). Some microscopic models suggest the involvement of grain boundaries [8], dislocation networks [9], a superglass phase [10], or a dislocation glass [11].

The goals of our study are twofold: first, the sample confinement is increased below 150 μm [6] to maximize the supersolid fraction. Second, we block annular cells with high NCRIs to test if these samples also exhibit the characteristic superflow behavior seen by KC.

We find that the supersolid fraction exhibits broad maximum of around 20% in narrow annuli of 100 μm. In such a cell, we confirm the blocked annulus result [1]: inserting a block in the flow path suppresses the supersolid fraction from 17.1% to below our experimental resolution of 0.8%.

In our latest design, we have constructed the torsion rod and the body of the torsional oscillator from the aluminum alloy 6061T6. Fig. 1 shows our aluminum torsional oscillator with an annular geometry. Its resonance frequency is 484.1 Hz at temperature $T = 4$ K with a quality factor, Q, of 5.3×10^5. The inner wall and torsion rod are made out of one piece to minimize the relative motion of the two constraining walls of the annulus. This design lessens the impact on the resonance period from ^{4}He shear modulus changes [12]. Another unique feature of our oscillator is that we can reversibly block it by introducing two rods that are centered in the annu-

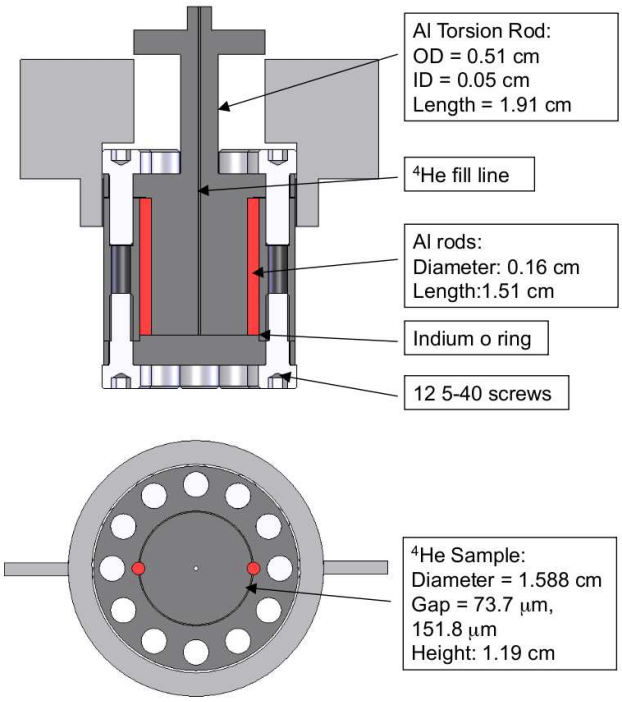

FIG. 1: Aluminum torsional oscillator with removable blocks (in red). The thin annular gap widths of 73.4 μm and 148.3 μm resulted in mass loading of 45.5 ns and 91.9 ns respectively. At 20 mK, the resonance frequency is 484.1 Hz and the quality factor of the oscillation is $Q \sim 5.3 \times 10^5$.

lus (diameter = 1.59 mm, shown in red in Fig. 1). This allows us to repeat KC's blocked annulus experiment [1] in thin cells with large supersolid fractions. The blocks also provide a mean to measure the moment of inertia of the solid, which is needed to compute supersolid fractions from the observed period drops. There are three configurations for the oscillator: first the blocked configuration with rods sealed in place; second,with slightly smaller diameter rods to maintain an annulus of constant width; and third with the rods absent, to study the effect on the NCRI of a larger region in the path of the superflow. We employ annuli with two different spacings, 73.4 μm, and 148.3 μm with surface to volume ratios (S/V) of 134.8 cm^{-1}, and 272.5 cm^{-1} respectively.

In most supersolid experiments, the total moment of inertia of the solid is determined by the period increase upon freezing. In small volume cells such as our narrow annuli, this increase is obscured by a simultaneous decrease due to the dropping pressure. In our experiment, a typical pressure drop of 30 bar in the cell during solidification results in a period drop of 60 ns. For the 73.4 μm cell, this drop exceeds the 45.5 ns period rise from solidification, making it impossible to use the standard experimental method. Alternatively, we can determine the solid inertia in our small volume cells by blocking the annulus: since the fluid backflow is negligible in thin annuli, a block in the flow locks the bulk liquid in the oscillator. When liquid enters the cell, two effects cause the resonance period to increase: the additional inertia stemming from the liquid ^{4}He as well as the cell's expansion due to the pressure. To separate pressure effects from the period change due to coupling of the liquid, we measure the resonance period as a function of liquid pressure in the cell. The extrapolation of the period to zero pressure is shifted with respect to the zero pressure measured period before the cell was filled. This period offset, ΔP, is the period change that stems from filling the cell with liquid at zero pressure. In order to calculate the period shift due to solid helium ΔP is rescaled by the ratio of solid to liquid density. The solid mass loadings in the 73.4 μm and 148.3 μm cells are 45.5 ns, and 91.9 ns respectively. All supersolid fractions are calculated by dividing the NCRI period drop by the solid mass loading.

We also use liquid ^{3}He in calibrating our cell. Here, we take advantage of the strong temperature dependence of the viscosity of liquid ^{3}He [13]. Above 100 mK, the viscosity is low and the fluid is mostly decoupled from the motion of the torsion bob. As the temperature is lowered, the viscosity increases and the fluid is increasingly locked in the annulus. The total fluid inertia can be determined independently from temperature and height of the dissipation maximum and from the period shift upon locking the liquid. The mass loadings determined with both methods differ by less than 5%.

Fig. 2 displays our main result of this series of experiments; the supersolid fractions are shown as a function

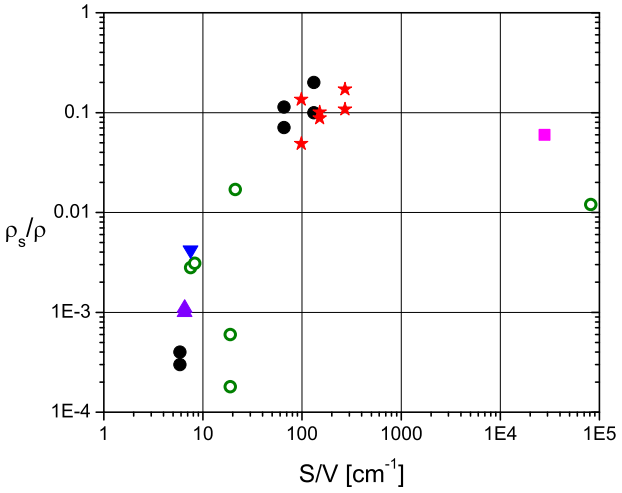

FIG. 2: The supersolid fraction, ρ_s/ρ, plotted as a function of the surface to volume ratio, which is inversely proportional to the annular width. The geometries for the different experiments from left to right are an open large cylinder (solid circles) [6], a cylinder (triangles) [3], two slightly different cylinders (open circles) [14], a cylinder (inverted triangle) [4], a welded annulus (open circles) [15], an annular cell (open circles) [2], thin annuli (solid circles and stars) [6], porous gold (square) [16], and smaller pore size porous gold (open circle) [16].

of S/V in different cells. In thin annular cells with gap, t, S/V simplifies to $\frac{2}{t}$. For large open geometries, the supersolid fraction is small, 0.03%. As we have reported before, the signal size increases dramatically by 3 orders of magnitude [6] with stronger confinement. In our latest data (solid stars), we find that the signals exhibit a broad maximum of around 20% at $S/V \sim 150$ cm^{-1}. When the sample is constrained further, the NCRI decrease back to $\approx 1\%$ for $S/V \sim 10^5$ cm^{-1}. Quench-cooling or annealing fail to alter the signal size.

Important information may be extracted from Fig. 2, particularly from the maximum NCRI and the length scale at which the maximum occurs. First, the maximum NCRI rules out the simplest explantation of superflow by a 3d network of grain boundaries. To see this, we employ Kosterlitz-Thouless theory of thin films. It relates the effective thickness of the grain boundaries and the observed transition temperature, T_c, via

$$t = k_B T_c \frac{2m^{*2}}{\pi\hbar^2 \rho_s} \qquad (1)$$

where k_B is the Boltzmann constant, m^* is the effective mass (here, the bare ^{4}He mass), $\hbar$ the reduced Planck constant and ρ_s is assumed to be the bulk density. For experimentally observed T_c's, this gives a grain boundary thickness on the order of tenths of Angstroms. Hence,

obtaining the observed 20% supersolid fraction would require an unphysical grain sizes on the order of 1 $\mathring{A}$. Possibly, a less simple version of the grain boundary theory might be reconciled with our observations.

Similarly, the maximum NCRI is difficult to reconcile with a dislocation network with superfluid cores. The measured dislocation density in a sample space with S/V = 2 cm^{-1} [17] is consistent with the expected supersolid signal of 0.1% in a similar geometry. On the other hand, a supersolid fraction, ρ_s/ρ, of 20% would require a dislocation density of 10^{13} cm^{-2} assuming a superfluid core of radius 6 $\mathring{A}$ [10]. This required density is three orders of magnitude higher than the highest measured dislocation density, corresponding to a spacing between dislocations of 3 nm. Consequently, it is improbable that this simple model can fully explain the supersolid results.

In a model that better accounts for the NCRI's geometry dependence, disorder is concentrated in a layer close to the walls [18]. This picture is consistent with the suggestion that dislocations form preferentially near cell walls in solid helium [19]. The surface roughness determines the penetration depth of the dislocation network, $\approx$ 1-5 μm for a polished metal surface. The maximal NCRI fraction is expected in an annular cell when the spacing is approximately twice the disordered layer thickness. Assuming that the supersolid fraction in the disordered region adjacent to the walls is 20%, we calculate the penetration depth to vary between 37 μm (current data) and 169 μm [6]. The penetration depth varies less between cells within the same series than between cells out of different materials. This larger variation may be related to the differences in the surface roughness.

The second goal of our experiments is to check if the high apparent supersolid fractions can still be attributed to long range superflow. For this reason, we repeat KC's blocked annulus experiment [1] in our narrow annular cells. In the blocked annulus experiment, a partition is placed across the annular channel, thus interrupting any long range flow around the annulus. The basic idea is to compare the magnitude of supersolid signals in an open and in a blocked annulus of the same width. In the experiments performed to date, the solid helium moment of inertia decreases upon blocking, indicating that the macroscopically coherent supercurrent is suppressed. As a minor caveat, there remains a small contribution to the NCRI from potential flow induced by the rotational motion of the oscillator. In the limit of a long narrow blocked channel, the NCRI from this backflow becomes negligibly small compared to the NCRI for the unimpeded flow in an unblocked channel. For example, in a 0.65 mm annulus, the period drop is reduced 200-fold [1]. Our annular width is 73.4 μm, more than an order of magnitude smaller than Kim and Chan's original cells (KC: open annulus gap = 0.95 mm, blocked annulus gap = 1.1 mm [20]) and the expected blocked annulus backflow NCRI is below our resolution.

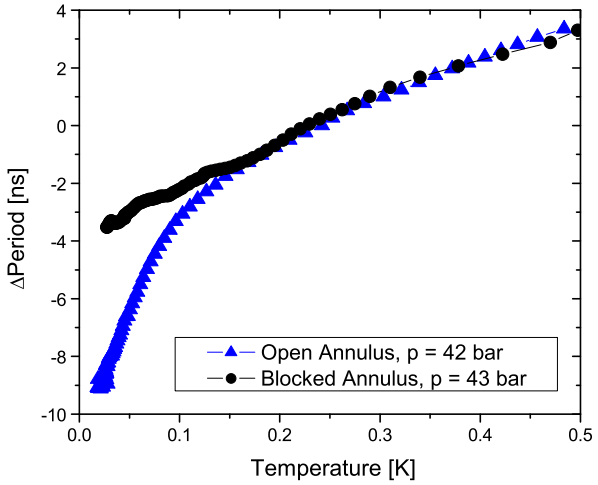

FIG. 3: Resonance period as a function of temperature in an open (solid triangles) and blocked (solid circles) annulus with a width of 73.4 μm. Both open and blocked annulus data are taken in the same cell which could be reversibly blocked (see Fig. 1). The nonclassical rotational inertia decoupling is 17.1% of the solid inertia in the open annulus. For the blocked annulus, the upper limit to the NCRI is 0.8% corresponding to a more than twentyfold reduction upon blocking.

Fig. 3 displays the resonance period as a function of temperature for both open and blocked annuli. Upon blocking the period drop at the supersolid transition is suppressed. Given the noise level of the experiment, the upper limit on a residual period drop in the blocked cell is $\sim$ 0.8%. The open cell displays a supersolid fraction of 17.1%, so the block suppresses the signal more than twentyfold. The major advantage of our setup with regard to KC's [1] is that our cell can be reversibly blocked, allowing one to measure open and blocked annuli within the same cell. We have also blocked a bigger annulus with a width of 487 μm and find the upper limit for a remnant supersolid signal to be 0.4%. In the open geometry, we expect the NCRI to be $\sim$ 5% (see Fig. 2).

Confirmation of the blocked annulus result demonstrates the nonlocal nature of the supersolid phenomenon. Thus, local models, such as the two-level tunneling systems [21], are unlikely to provide a full explanation of the supersolid.

We have also studied the effect of removing the rods and thus interposing a larger volume in series with the superflow. Although the fractional signal is smaller, $\sim$ 6%, the total mass current is not appreciably reduced.

Finally, we have measured the velocity dependence of the supersolid fraction below 40 mK [3, 20] in an annular cell with a 148.3 μm gap. Fig. 4 displays resonance period (solid circles) and dissipation (open circles) as a function

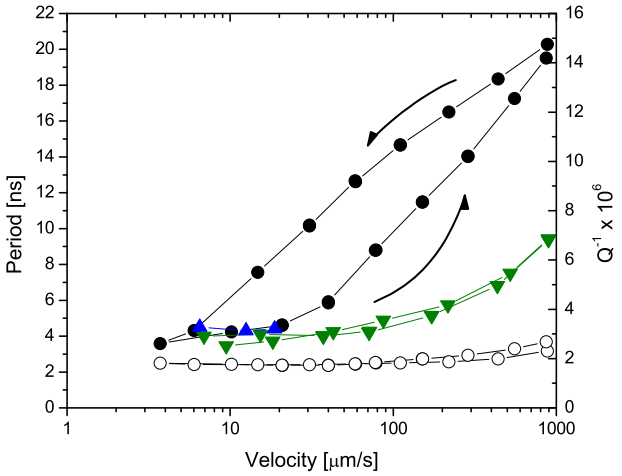

FIG. 4: Velocity dependence of resonance period (solid circles) and dissipation (open circles) at 20 mK in annular cell with a width of 148.3 μm. First, the sample is cooled at a high velocity, $v = 881$ μm/s, to 20 mK and then the drive is reduced at constant temperature. After reaching a low velocity, $v = 3.8$ μm/s, the drive is increased again. The critical velocity in this cell is $\sim$20 μm/s, as indicated by the low temperature period of cool downs at a constant drive level (triangles). We only show data points that were taken after the oscillator had time to equilibrate, about 20 minutes. Arrows indicate the direction of the velocity changes. For comparison, period data of the empty cell (inverted triangles) are displayed.

of rim velocity, v, at 20 mK. The empty cell background (inverted triangles) is displayed for comparison. Following a similar experimental procedure as [3], we cool the sample to 20 mK while oscillating at a high rim velocity, $v = 881$ μm/s. Holding the temperature fixed, the velocity is decreased in steps and then held for $\sim$ 20 minutes until the amplitude came into equilibrium as determined by the oscillator's Q. Starting from the lowest velocity $v = 3.8$ μm/s, we raise the velocity in steps. When the velocity surpasses ~ 20 μm/s, the period rises more steeply than the empty cell period, indicating that this cell's critical velocity has been exceeded. The period difference between cell filled with solid helium and empty cell at the highest velocity corresponds to a supersolid fraction of 12.0%. We observe some hysteresis between decreasing and increasing velocity, that is, the resonance period depends on the velocity history. In contrast, the resonance period shows no hysteresis at 60 and 200 mK.

Our finding differs from Aoki *et al.*'s observations in a cylindrical cell [3]. When their sample velocity increases, the NCRI stays constant above the critical velocity of 15 μm/s, up to 800 μm/s. Also in a cylindrical cell, Clark *et al.* [20] find a correlation between the sample growth method and the NCRI stability when the velocity is increased: constant pressure grown samples with relatively low NCRI are metastable at low temperatures, while the NCRI of blocked capillary grown samples is unstable against an increase in velocity. They attribute the existence of metastable states to severe vortex pinning in the sample at low temperatures, in qualitative agreement with Anderson's vortex liquid model [22]. The major difference between our experiments and other groups' lie in the annular geometry, stronger confinement and much higher supersolid fractions. Possibly, the smaller hysteresis in confined geometries can be attributed to the fact that vortices cross the sample more easily, for example because of a lower density of pinning centers.

We thank M.H.W. Chan, J.T. West, A.C. Clark, X. Lin, and E.J. Mueller for providing us with information about their torsional oscillators and extensive discussions, and we thank K.R.A. Hazzard for a critical reading of the manuscript. This work has been supported by Cornell University, the National Science Foundation under Grant DMR-060584 and through the Cornell Center for Materials Research under Grant DMR-0520404.

* Electronic address: ar297@cornell.edu

[1] E. Kim and M. Chan, Nature **427**, 225 (2004).
[2] E. Kim and M. Chan, Science **305**, 1941 (2004).
[3] Y. Aoki, J. C. Graves, and H. Kojima, Phys. Rev. Lett. **99**, 015301 (2007).
[4] M. Kondo, S. Takada, Y. Shibayama, and K. Shirahama, J. Low Temp. Phys. **148**, 695 (2007).
[5] A. S. C. Rittner and J. D. Reppy, Phys. Rev. Lett. **97**, 165301 (2006).
[6] A. S. C. Rittner and J. D. Reppy, Phys. Rev. Lett. **98**, 175302 (2007).
[7] S. Balibar and F. Caupin, J. Phys. Cond. Mat. **20**, 173201 (2008), N. V. Prokof'ev, Advances in Physics **56**, 381 (2007).
[8] L. Pollet, M. Boninsegni, A. B. Kuklov, N. V. Prokof'ev, B. V. Svistunov, and M. Troyer, Phys. Rev. Lett. **98**, 135301 (2007).
[9] M. Boninsegni, A. B. Kuklov, L. Pollet, N. V. Prokof'ev, B. V. Svistunov, and M. Troyer, Phys. Rev. Lett. **99**, 035301 (2007).
[10] M. Boninsegni, N. V. Prokof'ev, and B. V. Svistunov, Phys. Rev. Lett. **96**, 105301 (2006).
[11] A. V. Balatsky, M. J. Graf, Z. Nussinov, and S. A. Trugman, Phys. Rev. B **75**, 094201 (2007).
[12] J. Day and J. Beamish, Nature **450**, 853 (2007).
[13] J. M. Parpia, D. J. Sandiford, J. E. Berthold, and J. D. Reppy, Phys. Rev. Lett. **40**, 565 (1978).
[14] A. C. Clark, J. T. West, and M. H. W. Chan, Phys. Rev. Lett. **99**, 135302 (2007).
[15] J. T. West, *private communication.*
[16] E. Kim and M. H. W. Chan, J. Low Temp. Phys. **138**, 859 (2005).
[17] F. Tsuruoka and Y. Hiki, Phys. Rev. B **20**, 2702 (1979).
[18] K. R. A. Hazzard, *private communication.*
[19] Y. Kosevich and S. Svatko, Fiz. Nizk. Temp. **9**, 193

(1983).
[20] A. C. Clark, J. D. Maynard, and M. H. W. Chan, Phys. Rev. B **77**, 184513 (2008).
[21] A. Andreev, JETP Lett. **85**, 585 (2007).
[22] P. W. Anderson, Nature Physics **3**, 160 (2007).